Doppler-Free Spetroscopy of Rubidium

Pranjal Vachaspati, Sabrina Pasterski*
MIT Department of Physics
(Dated: April 17, 2013)

We present a technique for spectroscopy of rubidium that eliminates doppler broadening. Using this, we probe the hyperfine structure of rubidium and determine the hyperfine coupling constants. We find for ^{85}Rb a coupling constant of 973 ± 21MHz in the $5S_{1/2}$ state and constants of $A = 24 \pm 2$MHz, $B = 22 \pm 2$ for the $5P_{3/2}$ state. We find for ^{87}Rb a coupling constant of 3260 ± 60MHz in the $5S_{1/2}$ state and constants of $A = 83 \pm 8$MHz, $B = 14 \pm 1$ for the $5P_{3/2}$ state.

I. INTRODUCTION

Spectroscopy is a powerful technique that is widely used for an enormous range of purposes. Here we present an application of atomic spectroscopy to verify results from theoretical quantum mechanics. Theoretical knowledge of the structure of the atom predicts a series of refinements to the energy spectrum of a hydrogen-like atom such as rubidium. Naïve spectroscopy fails to probe this spectrum to a satisfactory degree due to doppler broadening effects, so a hole-burning technique is applied to eliminate those effects. By doing so, we can confirm quantum mechanical results and measure quantitative properties of the rubidium atom.

II. THEORY

II.1. Doppler-Free Absorption Spectroscopy

Absorption spectroscopy provides a method for determining transitions between energy levels of a material. A quantum system can absorb only excitations that allow it to transition from one energy eigenstate to another. By exciting the system with a range of energies, we can detect which are absorbed, determining the spacings in the energy levels of the material.

In this case, we excite a gas of rubidium atoms with a near-infrared laser. Because the gas has a wide velocity distribution, particles in the gas experience a range of doppler shifts, so a sharp laser line appears as a broad line to the gas, obscuring certain spectral features. To remove this doppler broadening, a technique known as hole-burning is used. A strong pump beam with frequency ν is sent through the cell in one direction, exciting atoms with velocity such that $\nu_{transition} = \left(1 + \frac{v}{c}\right)\nu$, removing them from the ground state. At the same time, a weak "probe beam" with the same frequency is sent through the cell in the *opposite* direction, exciting atoms with velocity such that $\nu_{transition} = \left(1 - \frac{v}{c}\right)\nu$.

When the laser is close to, but not very close to the transition frequency, the probe and pump excite different groups of atoms, and the probe beam shows a normal doppler-broadened spectrum. However, when the laser is tuned very close to the transition frequency, the pump beam depopulates the state that the probe beam tries to excite. This creates a "Lamb dip" in the absorption spectrum, as there are no ground-state atoms left for the probe beam to excite. Measuring the size and location of the Lamb dip allows more precise determination of the absorption spectrum.

II.2. Rubidium Spectrum

Rubidium has one valence electron, so its electron energy levels resemble hydrogen[5]. As with hydrogen, the roughest approximation of the spectrum ignores spin and relativistic effects, specifying the $n = 1, 2, \ldots$ states. Here, we do not probe transitions between these states. Instead, we examine first and second order perturbations to the ground state.

The first perturbation (the fine structure) comes from spin-orbit interactions. This splits the ground state into states that depend on the electron angular wavefunction. The ground state is specified in Russell-Saunders notation[3] as $5^2S_{1/2}$, and the first two excited states are $5^2P_{1/2}$ and $5^2P_{3/2}$. The transition we probe here is between the ground state and the $5^2P_{3/2}$, which occurs at 780 nm.

This transition is further perturbed by the nuclear spin, causing hyperfine splitting. ^{87}Rb has a nuclear spin of $I = 3/2$ and ^{85}Rb has a nuclear spin of $I = 5/2$. This splits the ground state into two levels with total angular momentum $F = 1$ and $F = 2$ in the case of ^{85}Rb, and

* pranjal@mit.edu, fermilab@mit.edu

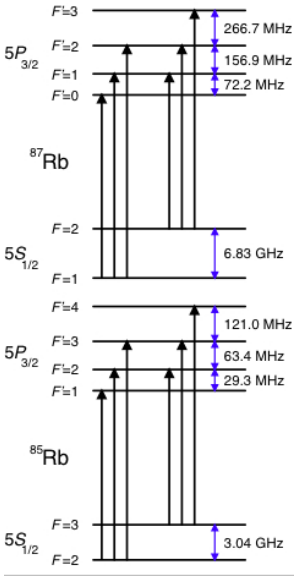

FIG. 1. Nuclear spin effects cause hyperfine splitting, which splits each electron angular wavefunction into separate energy levels[4].

with $F = 2$ and $F = 3$ in the case of ^{87}Rb. It also splits the excited state into four levels, with momenta $F = 0, 1, 2, 3$ in the case of ^{85}Rb, and $F = 1, 2, 3, 4$ in the case of ^{87}Rb.

A selection rule limits transitions to a change in angular momentum of at most 1, so there are three transitions between each ground state splitting and the excited state. The hyperfine splittings for the ground state are 10 to 100 times larger than for the excited state, so this gives four clusters (two per isotope) of three transitions each, for a total of twelve peaks in the spectrum. The transition frequencies are given by

$$\nu_F = \nu_J + A\frac{C}{2} + B\frac{\frac{3C(C+1)}{4} - I(I+1)J(J+11)}{2I(2I-1)J(2J-1)} \quad (1)$$

where $C = F(F+1) - J(J+1) - I(I+1)$, ν_J is the fine frequency, and A, B are experimentally determined constants.

The energy level diagram for the hyperfine splittings of this transition is given in 1.

II.2.1. Crossover Peaks

Lamb dips can also occur when the laser is not at a transition frequency. In each cluster of transitions from a single ground state, when the laser is halfway between two transitions, the pump beam will depopulate the ground state into one excited state, while the probe beam will attempt to excite into a different excited state. This still creates a Lamb dip, since the ground state is depopulated even though the pump and probe are exciting slightly different transitions.

II.3. Resonating Cavities

Optical resonating cavities are critical to measuring and determining the laser wavelength. An optical cavity consists of two very parallel semi-transparent mirrors between which a standing wave can develop. Such a cavity with length ℓ and refractive index n will amplify only light with wavelength $m\lambda = 2n\ell$, for integer m. Thus, the free spectral range of a cavity, given as the spacing between adjacent peaks, is given by

$$\Delta\nu = \frac{c}{2nL} \quad (2)$$

II.4. Diode Laser

A diode laser is used to excite the rubidium atoms used in this experiment. Diode lasers use semiconductors as the lasing medium. A standard semiconductor diode consists of the interface between a P-doped semiconductor and an N-doped semiconductor. When unbiased, the interface becomes a "depletion region" as the holes from the P-doped region combine with electrons from the N-doped region to form a layer with no mobile charge carriers but a net electric field.

When an external voltage is applied that cancels out this electric field, electrons and holes can diffuse across the junction. At the interface, electrons and holes combine, releasing energy. In an "indirect bandgap" semiconductor like silicon, this energy change corresponds to a momentum change, and most of the energy is released as heat. However, in a "direct bandgap" semiconductor like aluminum gallium arsenide, the energy change does not change the momentum, and the combination of the charge carriers releases a photon instead. This creates a light-emitting diode (LED).

The LED is turned into a laser with the addition of parallel semi-reflecting surfaces on the sides of the diode. The photons which are reflected back into the semiconductor cause simulated emission when they are absorbed by charge carriers, which recombine and emit two coherent photons. The wavelength of the laser can be changed by changing the temperature and power go-

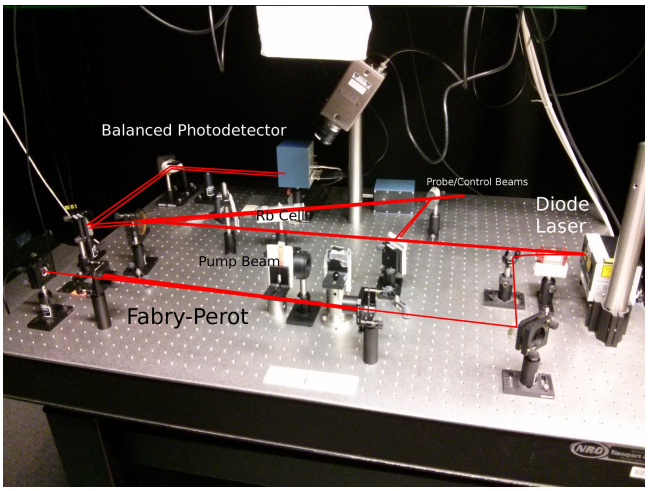

FIG. 2. The beam is split twice, first to measure frequency changes with the Fabry-Perot interferometer, then into probe, pump, and control beams to measure the spectrum.

ing to the diode, which change the size and refractive index of the diode.

III. EQUIPMENT & PROCEDURE

III.1. Overview and Beam Path

The optical table and beam path are shown in Figure 2. The diode laser passes through an optical isolator, which protects the laser and reduces the likelihood of mode-hopping, and then is split twice. First, a small fraction of the beam is reflected off a glass plate into the Fabry-Perot interferometer (III.4) to measure frequency changes. Then, the beam passes through a prism which refects a small portion of the light twice, to form the pump, probe and control beams. A balanced photodetector (III.3) measures the difference between the probe and control beams to get the spectrum.

III.2. Diode Laser Package

We use a commercial TUI external cavity diode system with a AlGaAs laser head[2]. An externally mounted diffraction grating is pivoted by a servomotor to act as a wavelength-selective mirror. This allows a frequency sweep of around 10 GHz - approximately 1 nm with a linewidth of around 30 MHz.

III.3. Balanced Photodetector

As seen in Figure 2, the pump beam travels through the cell in the opposite direction as the probe and control beams. The pump beam and the probe beam travel through the same region, allowing the probe beam to measure a spectrum with Lamb dips, while the control beam does not intersect the pump beam, ensuring that the control beam measures only a doppler-broadened spectrum.

A balanced photodetector[1] contains two photodiodes that measure the intensity of both the probe and control beam, then subtracts them to determine a spectrum of only Lamb dips, allowing the observation of the hyperfine splitting.

Since various factors could shift the relative intensity of the beams, it was sometimes necessary to take successive measurements with the pump beam blocked and unblocked, and subtract them afterwards to get the best possible spectrum.

III.4. Fabry-Perot Interferometer

The relative wavelengths of the laser are determined with a Fabry-Perot interferometer. This is a optical cavity as described in II.3, with two partially reflecting mirrors separated by 47.1 ± 0.7 cm. This distance is measured by placing a ruler in the same plane as the cavity and counting pixels in a digital photograph of the scene. Such a cavity has a free spectral range of 318 ± 5 MHz. Uncertainties in this measurement come from the pixel precision of the camera and from uncertainty in the precise mirror position in the mirror mount, as well as the fact that light might bounce off both sides of the mirror

IV. RESULTS

A full spectrum showing all four clusters of transitions is shown in Figure 3. The ground state hyperfine splittings can be determined by measuring the distance between the clusters, and the excited state splittings can be determined by measuring the distances between peaks in the individual clusters.

A fit to the zero-crossings in the Fabry-Perot output, as shown in Figure 4, allows for interpolation to determine peak frequencies to a high degree of precision. Ideally, the laser would have a linear frequency ramp, but it is significantly better described by a slightly quadratic

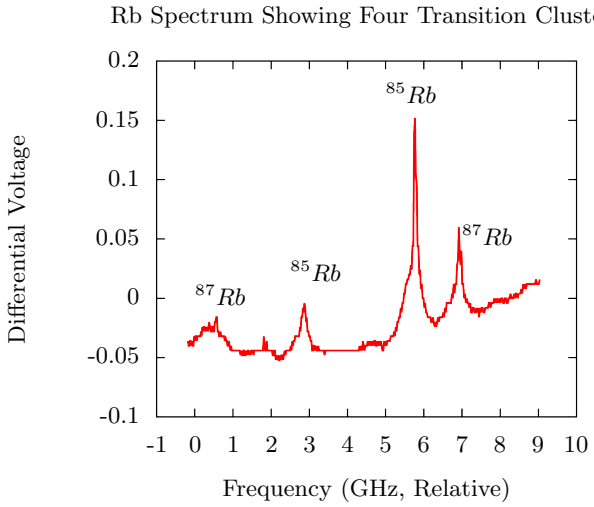

FIG. 3. A full spectrum taken over approximately 8 GHz shows four clusters of transition peaks corresponding to the split ground states of ^{85}Rb and ^{87}Rb. From this graph the splitting constants of the $5S_{1/2}$ ground state can be derived.

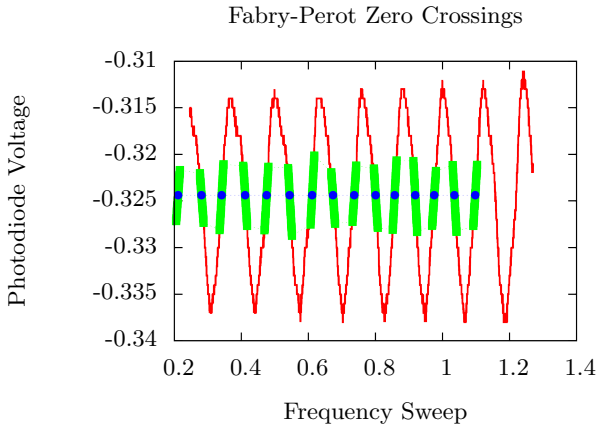

FIG. 4. The Fabry-Perot outputs a sinusoidal signal that can be converted to a relative frequency measurement by locating and fitting to the zero-crossings.

ramp, indicating that the laser scans slightly faster towards one end of the ramp.

The peaks are then located by a quadratic fit to the area around the peak. From the full spectrum in Figure 3, we find splittings of 2920 ± 64 MHz for ^{85}Rb and 6520 ± 120 MHz for ^{87}Rb.

Both these values slightly underestimate the known value of the splittings, which are 3040 MHz and

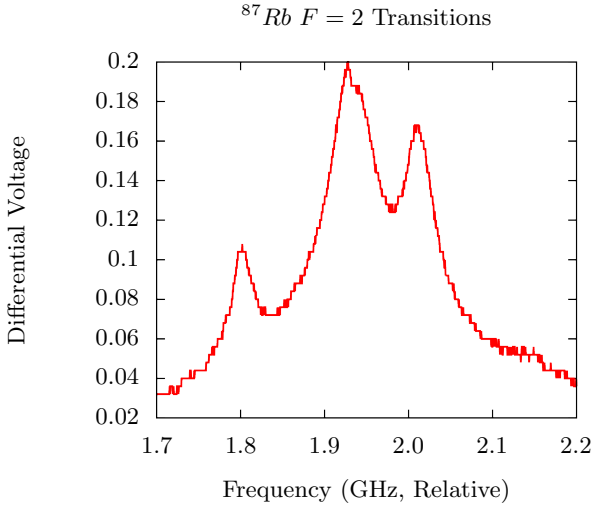

FIG. 5. A slow sweep over a smaller frequency range allows precise measurement of transitions from a single ground state. The polarity of the signal is arbitrary and depends on the configuration of the balanced photodetector. Only the lowest energy transition and crossover peaks are visible in this region.

6830 MHz respectively.

Next, the laser is swept more slowly over small regions to determine the splittings of the first excited state. For most of these transitions, the crossover peaks are much more visible than the normal transition peaks, so the frequency differences between the peaks must be doubled to find the actual transition frequencies. This method gives spacings of 262 ± 10 MHz and 151 ± 16 MHz for the two higher ^{87}Rb frequencies, and spacings of 113 ± 6 MHz, 62 ± 4 MHz for ^{85}Rb. These agree with the accepted values of 266.7 MHz, 159.6 MHz, 121.0 MHz, and 63.4 MHz.

From these spacings and equation 1, we can derive the coupling constants for each of the rubidium states. For the $5S_{1/2}$ state, we find $A = \frac{\Delta\nu}{C_{F=3}-C_{F=2}} = \frac{\Delta\nu}{3} = 973 \pm 21$MHz for ^{85}Rb and $\frac{\Delta\nu}{2} = 3260 \pm 60$MHz for ^{87}Rb. These both underestimate the accepted values of 1011 MHz and 3417 MHz, which is discussed in V. Analagously, we derive for the $5P_{3/2}$ state $A = 83 \pm 8$MHz, $B = 14 \pm 1$MHz for ^{87}Rb, and $A = 24 \pm 2$MHz, $B = 22 \pm 2$MHz for ^{85}Rb. These numbers agree with the accepted values of $A = 84.7, B = 12.5$ for ^{87}Rb, and $A = 25.0, B = 25.7$ for ^{85}Rb at approximately one standard deviation.

V. ERRORS

The errors in this measurement are derived from a combination of resolution limitations of the voltage measuring devices and noise in the experiment, as well as statistical error between runs.

When measuring the full spectrum, the time resolution of the oscilloscope and scan speed of the laser controller allowed us only 20 MHz resolution, limiting the fidelity with which the peak could be detected. Furthermore, errors in the measurement of the Fabry-Perot length as described in III.4 accumulated over the large wavelength differences to arrive at the total wavelength estimate.

The underestimate of the ground state splitting can be explained by carefully examining the energy level diagram (1). The resolution of the full spectrum is only good enough to fit to each of the four clusters, not to the individual transitions themselves. This means that the two peaks measured for ^{87}Rb represent the $F = 1 \rightarrow F' = 1$ and $F = 2 \rightarrow F' = 2$ transitions. However, the splitting that must be measured is between the $F = 1 \rightarrow F' = 2$ peak and the $F = 2 \rightarrow F' = 2$ peak. To correct for this, the splitting between the $F' = 1$ and $F' = 2$ levels can be added to the measured frequency, producing results that better match the known values, but are still slightly low.

Fitting the peaks was also challenging for the excited state splittings. Stray reflections in the rubidium cell could cause Lamb dips to appear in the control beam, causing dips within dips in the subtracted spectrum. As a result, it was sometimes difficult to determine which section of a peak was the real peak of the Lamb dip.

The errors are significantly larger in the ^{87}Rb spectrum compared to ^{85}Rb; this is because ^{85}Rb is roughly 2.5 times more prevalent and therefore gives a stronger signal.

VI. CONCLUSION

We find values for the coupling constants that agree for the most part with accepted values; where they do not, we theorize that the measured values actually measure a slightly different attribute of the spectrum, which can be corrected for to give values that agree more closely with the accepted figures.

[1] *MIT Balanced Detector.*
[2] *Tui-Optics Laser System Brochure: DL100.*
[3] MIT Department of Physics. Doppler-free spectroscopy. November 2012.
[4] G.T. Purves. Rubidium d2 line data, 2005.
[5] Daniel A Steck. Rubidium 87 d line data, 2010.
[6] Daniel A Steck. Rubidium 85 d line data, 2012.